LUNG SEGMENTATION OF X-RAY THORAX IMAGE USING GEOMETRIC ACTIVE CONTOUR AND ENHANCEMENT SPATIAL DOMAIN FILTERING

Mokhamad Amin Hariyadi
Informatic Engineering Department, Faculty of Science and Technology,
Islamic State University Maulana Malik Ibrahim Malang - Indonesia

e-mail : adyt2002[at]gmail.com

ABSTRACT

Chest cavity is an important part of the body structure because there are vital organs in it, namely the lungs. The lungs are the organs that come into contact with the outside of the body, where the disturbances in this organ could have implications for other vital organs, therefore it is necessary for clinical examination and x-ray examination.
So far, the observations of lungs from the x-ray image of the thorax have been done manually by a physician or radiologist, the results obtained are generally subjective. Therefore, it is needed to have medical aids that can provide a better analysis and used in various things, such as mass screening thorax. In this research, an application for segmenting lungs from the thorax x-ray image is developed using geometric active contour and enhancement spatial domain fitering.
This study used 45 X-ray images of the chest cavity (thorax). Results of performance testing in the geometric active contour segmentation, it is obtained: accuracy of 95.2%, sensitivity of 70.4% and specificity of 99.8% for the average right and the left lungs.

KEYWORDS

enhancement spatial domain, geometric active contour

1. INTRODUCTION

Chest cavity is an important part of the body structure because there are vital organs in it, namely the lungs. The lungs are the organs that come into contact with the outside of the body, where the disturbances in this organ could have implications for other vital organs. One way to determine an abnormality or disturbance in the chest cavity is based on clinical symptoms and examination of the x-ray thorax [1]. Several medical studies show the condition of lungs can be used as a parameter identification of early cardiac abnormalities.

So far, the observations of lungs from the X-ray image of the thorax have been done manually by a physician or radiologist, the results obtained are generally subjective due to the results of x-ray image of the thorax are affected by overlapping objects that are not the concern. To overcome these problems, we need a technology that is able to show clearly the information as needed, by digital image processing. Processing of x-ray images is carried out in several stages; segmentation stage is the most important for effective segmentation will increase the likelihood obtainment of good diagnostic results [2].

Research carried out by Bram [3][4] and some previous researchers used the methods divided in rule-based (RB) and pixel classication (PC) schemes with 94% accuracy rate of 115 x-ray image of the thorax observed. The results of this study provide many significant additional values, particularly in the areas of segmentation of lung x-ray image of the thorax.

Level of accuracy obtained from the previous studies still need to be improved in order to obtain better medical diagnosis results, and then this study proposes geometric active contour method to generate a good level of accuracy. This method has an ability to minimize area-based energy, so that the movement of the curve in the segmentation process is better and more effective.

2. MATERIAL AND METHODS

Methods used in this research can be broadly described by using the stages as shown in Figure 1.

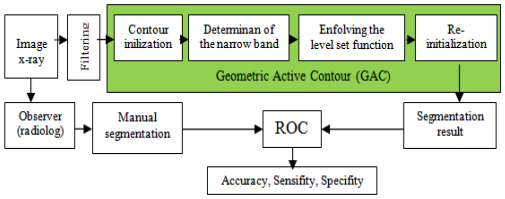

Figure 1. Research design

2.1. X-ray image

In general, the results of x-ray image shows the structure of organs on the chest have in common, good shape, size and the location, so it is quite difficult to be seen by naked eye whether there is an abnormality of the organs, it would require a special expertise in the readings. This study used 45 x-ray thorax image results and with the manual segmentation results that had been validated, the data were retrieved from the public database [5]. Furthermore, changes were made to the format of the required image, then the image of x-ray was segmented using geometric active contours.

2.2. Enhancement spatial domain (ESD)

Enhancement spatial domain filtering is used in the repair of the digital image results by adjusting levels of brightness and contrast. This is done by assuming brightness variation on the digital image as a histogram of the image, and how an image can be manipulated by changing the existing histogram to the normal distribution.

Histogram will put the existing pixels with brightness levels corresponding provision (having similarity) So that, the histogram which has a smaller brightness value will appear darker than the larger value [6].

2.3. Geometric active contour (GAC)

Geometric active contour [7], which is known as deformable models, is a collection of some moving points approaching the limits of an object. Its movement is described as a number of control points which follow each other, so that the necessary provision of the estimated initial contour is assumed nearly approximate to the shape of the object features. Then, the contour will be attracted towards the feature inside the image due to the influence of the energy produced by object features.
To detect a form of an object of this image method, the way the movement of the curve is used. The curve is drawn repeatedly by the limitations of the given image, so that the shape of the object from the image can be detected. Geometric active contour requires very much computing, yet it has the advantage that can automatically handle the topology changes beyond parametric active contour since the method has the ability to minimize the area-based energy [8].

2.3.1. Contour initialization

Specifying a polygonal region of interest (ROI) within an image can be done by using Roipoly function. Roipoly has a function to return a binary image which can be used as a mask for masked filtering.

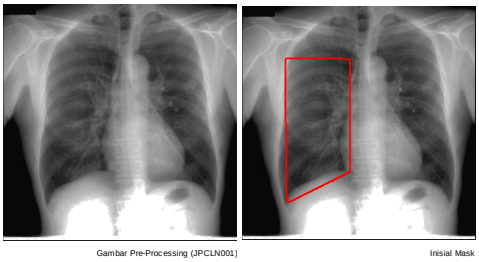

(a) (b)

Figure 2. (a) image input, (b) contour initialization output

2.3.2. Narrow Band

Narrow Band is a way to accelerate the calculating process of the curve movement. This method works by simply counting the pixels that are located adjacent to the curve initialization as illustrated in Figure 3.

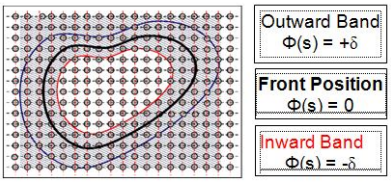

Figure 3. Curve function with narrowband [8]

2.3.3. Compute c_1 dan c_2

By providing value ϕ and minimizing energy $F(c_1, c_2, C)$ so we can calculate the average intensity using the function:

$$c_1(\phi) = \frac{\int_\Omega u_0(x,y)H(\phi(x,y))dx\,dy}{\int_\Omega H(\phi(x,y))dx\,dy}$$

$$c_2(\phi) = \frac{\int_\Omega u_0(x,y)\left(1 - H(\phi(x,y))\right)dx\,dy}{\int_\Omega \left(1 - H(\phi(x,y))\right)dx\,dy}$$

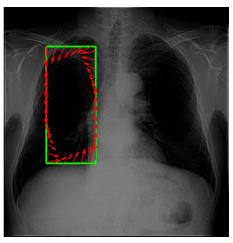

Figure 4. Contour initialization of the narrow band with C_1 and C_2.

2.3.4. Contour moving

Based on the definition of the energy function of the model can be written as a function ϕ according to the Euler-Lagrange equation as follows:

$$\frac{\partial \phi}{\partial t} = \delta(\phi)[\mu\, k(\phi)|\nabla\phi| - v - \lambda_1(u_0 - c_1)^2 + \lambda_2(u_0 - c_2)^2]$$

where :

$$k(\phi) = \frac{\phi_{xx}\phi_y^2 - 2\phi_{xy}\phi_x\phi_y + \phi_{yy}\phi_x^2}{\left(\phi_x^2 + \phi_y^2\right)^{3/2}}$$

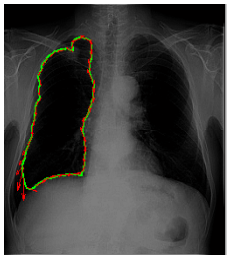

Figure 5. Contour moving

2.3.5. Re-initialization

The segmentation process of geometric active contour method has both internal and external energy, where the initialized contour will evolve and move closer to the edge image as the effects of both energies. The result of the evolution is a gradient flow of the image which has minimum value of the overall energy function. Segmentation process produces output data in the form of lungs contour.

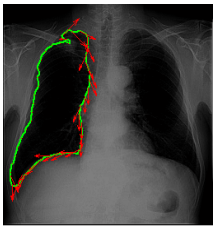

Figure 6. Contour re-innitialization

2.4. Reciever operating characteristic (ROC)

The results of the detection of lung level set segmentation is then compared to the results of manual segmentation, using the ROC. From the comparison of the investment, it would be worth TP: True Positive, FN: False Negative, TN: True Negative, and FP: False Positive, which is calculated based on the number of pixels covered.

The results of the level set segmentation are converted to the Black-White level, all pixels in the form of pulmonary organ is set to black, while the non-lung pixels in all are in white. This process is done by finding the inverse image.

Value of TP, FN, TN and FP are calculated based on Figure 4. Where TP is a lung pixel and recognized as lung, FP is a non-lung pixel yet recognized as a lung, FN is the lung pixel but not recognized as the lung, and TN is not a lung pixel and not recognizable as lung.

These four values can be formulated using 2 x 2 matrix as follows:

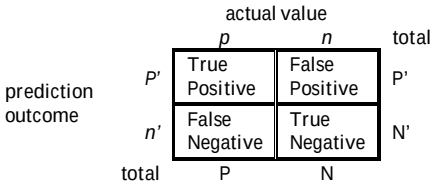

Figure 7. Matrix formulation of TP,TN,FP,FN[9]

Based on those values, it can measures the sensitivity, accuracy and specificity values.

3. RESULTS

The calculation results of accuracy, sensitivity and specifity of lung segmentation using GAC methods can be seen in Table 1.

Table 1. Data of accuracy, sensitivity and specifity of image segmentation results for both right and left lungs.

No	Image	Left Lung(%)			Right Lung (%)		
		Accuracy	Sensitivity	Specificity	Accuracy	Sensitivity	Specificity
1	'JPCLN0_1.jpg'	95.3	88.2	99.8	95.0	68.7	99.8
2	'JPCLN0_10.jpg'	93.8	82.1	100.0	93.9	50.5	99.6
3	'JPCLN0_11.jpg'	96.8	64.5	100.0	96.6	81.1	99.3
4	'JPCLN0_12.jpg'	92.7	74.8	100.0	96.7	79.4	99.8
5	'JPCLN0_13.jpg'	95.3	64.3	100.0	96.4	74.8	99.7
6	'JPCLN0_14.jpg'	95.2	77.5	99.9	94.9	66.9	99.9
7	'JPCLN0_15.jpg'	95.8	88.0	99.9	94.6	64.8	99.7
8	'JPCLN0_16.jpg'	96.9	71.7	99.2	94.6	79.1	96.6
9	'JPCLN0_17.jpg'	94.0	66.6	100.0	96.0	71.2	99.7
10	'JPCLN0_18.jpg'	95.0	81.4	100.0	94.7	82.0	97.9
11	'JPCLN0_19.jpg'	94.9	77.8	99.8	95.5	71.0	99.9
12	'JPCLN0_2.jpg'	96.7	72.6	99.8	97.6	79.9	99.8
13	'JPCLN0_20.jpg'	95.0	64.6	100.0	94.0	61.9	99.7
14	'JPCLN0_21.jpg'	96.4	75.3	100.0	96.7	78.5	99.8
15	'JPCLN0_22.jpg'	93.6	67.8	100.0	93.6	59.3	99.9
16	'JPCLN0_23.jpg'	94.1	64.4	100.0	94.2	67.9	99.3
17	'JPCLN0_24.jpg'	95.6	64.0	100.0	95.1	64.9	99.9
18	'JPCLN0_25.jpg'	93.2	69.1	100.0	95.8	61.0	99.9
19	'JPCLN0_26.jpg'	94.2	74.7	99.9	95.2	69.6	99.8
20	'JPCLN0_28.jpg'	95.2	71.8	100.0	95.7	76.3	99.2
21	'JPCLN0_29.jpg'	95.2	64.0	99.3	95.8	66.6	99.3
22	'JPCLN0_3.jpg'	95.7	72.1	99.9	96.2	71.0	99.4
23	'JPCLN0_30.jpg'	95.4	88.2	99.8	94.5	56.8	99.9
24	'JPCLN0_31.jpg'	93.6	82.1	100.0	93.8	58.6	100.0
25	'JPCLN0_33.jpg'	98.0	64.5	100.0	97.1	77.4	99.6
26	'JPCLN0_35.jpg'	96.3	74.8	100.0	96.1	78.7	99.8
27	'JPCLN0_37.jpg'	94.4	64.3	100.0	95.0	58.1	100.0
28	'JPCLN0_38.jpg'	96.3	77.5	99.9	97.6	83.2	99.8
29	'JPCLN0_39.jpg'	93.9	88.0	99.9	93.8	55.5	100.0
30	'JPCLN0_40.jpg'	95.1	71.7	99.2	93.6	65.6	99.9
31	'JPCLN0_41.jpg'	97.9	66.6	100.0	97.0	83.9	99.2
32	'JPCLN0_42.jpg'	95.7	81.4	100.0	95.2	56.9	99.7
33	'JPCLN0_43.jpg'	94.4	77.8	99.8	94.7	62.8	99.8
34	'JPCLN0_45.jpg'	95.8	72.6	99.8	94.7	68.3	99.9
35	'JPCLN0_46.jpg'	96.0	64.6	100.0	95.6	74.8	99.7
36	'JPCLN0_47.jpg'	94.6	75.3	100.0	96.0	78.5	99.0
37	'JPCLN0_48.jpg'	95.0	67.8	100.0	96.3	59.4	99.7
38	'JPCLN0_49.jpg'	94.8	64.4	100.0	95.4	70.6	100.0
39	'JPCLN0_5.jpg'	95.1	64.0	100.0	96.7	73.5	99.5
40	'JPCLN0_50.jpg'	93.9	69.1	100.0	94.7	61.3	99.9
41	'JPCLN0_6.jpg'	94.2	74.7	99.9	94.6	63.3	99.9
42	'JPCLN0_62.jpg'	94.0	71.8	100.0	94.9	62.5	99.9
43	'JPCLN0_7.jpg'	95.0	64.0	99.3	93.9	62.2	99.8
44	'JPCLN0_8.jpg'	93.7	72.1	99.9	94.5	70.9	99.9
45	'JPCLN0_9.jpg'	93.0	88.2	99.8	94.4	61.3	99.8
Rata-rata		**95.1**	**72.1**	**99.9**	**95.3**	**68.7**	**99.6**

Image column describes x-ray image used in the study, accuracy, sensitivity, specificity columns describe the level of accuracy, sensitivity and specificity of the results of geometric active contour with manual (gold standard). The average is the total value of the overall observations and divided by the number of observations.

Table 1 shows that the highest level of accuracy is 97.6% (JPLN0_2) and the lowest level of accuracy is 93.6% (JPLN0_21, JPLN0_40) for the right lung, meanwhile the highest level of accuracy of the left lung is 98%(JPLN0_33) and the lowest level of accuracy is 93%(JPLN0_9).

ISBN: 978-0-9891305-5-4 ©2014 SDIWC

Table 2. Accuracy, Sensitivity and Specificity of study using GAC-ESD method, K-means-GAC and GVF snake for both right and left lungs

Methods	Value (%)		
	Accuracy	Sensitivity	Specificity
GAC–ESD, right	95.3	68.7	99.6
GAC–ESD, left	95.1	72.1	99.9
Average	95.2	70.4	99.8
GAC unpre-processing, right	92.3	56.5	99.9
GAC unpre-processing, left	93.4	54.3	99.8
Average	92.9	55.4	99.8
K-means-Level sets, right	88.4	63.7	93.5
K-means-Level sets, left	90.0	62.1	94.6
Average	89.2	62.9	94.1
GVF snake, right	94.3	73.3	98.0
GVF snake, left	94.5	72.9	98.4
Average	94.4	73.1	98.2

The left column of the table describes the methods used in the study, while the column of sensitivity, accuracy and sensitivity describes the results obtained from each method. For column left (%) and right (%) describes the left lung and right lung.

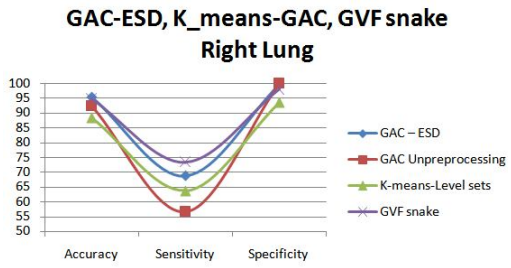

(a)

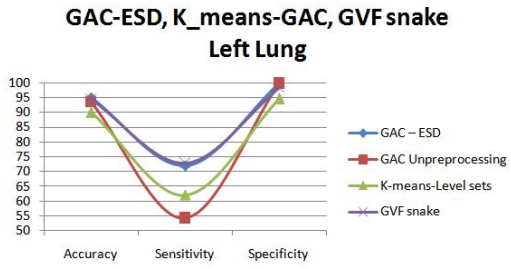

(b)

Figure 8. (a). Graph comparison GAC-GAC-AHE K_means and GVF snake for the left lung, (b). Graph comparison GAC-GAC-ESD, K_means and GVF snake for the right lung.

Table 2 and Figure 8 (a)(b) show the segmentation results of geometric active contour method which has average level of accuracy of 95.2% for both the right and left lungs.

4. DISCUSSION AND CONCLUSION

4.1. Discussion

Geometric active contour method on level set function and chan vase, the initial contour initialization phase is very influential in the evolution process and the obtained results, in this method the initial contour initialization which is closer to the object feature will obtain the expected output and the number of evolution and iteration will be shorter. (Fig. 6)

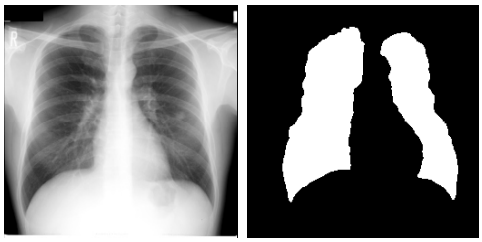

a b

Figure 9. (a) x-ray input, (b) output geometric active contour

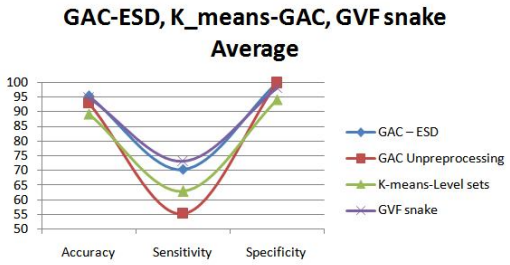

Figure 10. Graph comparison GAC-GAC-AHE K_means and GVF snake

Segmentation geometric active contour which obtained average accuracy of 95.2%, 70.4% sensitivity, and 99.8% specificity clearly proves that this method is better than previous methods.

These results show that, this method can be used to perform lung segmentation from x-ray thorax image; it is evident from the results of an accuracy of 95.2% which indicates the level of compliance with the segmentation performed by radiologists.

4.2. Conclussion

The results of this comparison shows that the level of accuracy, sensitivity and spesifitasi of GAC-ESD method have high values, compared with the K-means-GAC and GVF - Snake, for the right and left lung.

REFERENCES

[1] Fatchoerochman, Zulqarnain, N., Kuntjoro, E., 2010, Radiation Pneumonitis Incidents to Breast Carsinoma Patient Having Chemoradiation Therapy in RSSUP Dr. Kariadi, Radiology Unit Medical Faculty UNDIP, SUP. Dr. Kariadi Semarang.

[2] Rafsyam, Y., 2008, USG Image Segmentation Methode for Cyst Detection, Thesis, Electrical Engineering Department Gajah Mada University, Yogyakarta.

[3] Arnold M.R. Schilhm, B. van Ginneken, Marco Loog., 2005, A computer diagnosis system for detection of lung nodules in chest radiographs with an evaluation on public database.

[4] Bram van Ginneken, Mikkel B. Stegmann, and Marco Loog, 2006, Segmentation of anatomical structures in chest radiographs using supervised methods: a comparative study on a public database, 11th

[5] Image Sciences Institute Research Databases. http://www.isi.uu.nl/Research/Databases/.

[6] Balza, A. & Katika F. 2005, Digital Image Processing Using Delphi, Ardi. Yogyakarta.

[7] Lailyana, E., 2009, Lungs Segmentation of X-ray Image using Level Set, Thesis, Electrical Engineering Department Faculty of Industrial Technology Tenth November Institute of Technology, Surabaya.

[8] Chan, T., Vese, L., 2001, Active Contour Without Edges. IEEE Transaction on Image Processing, Vol.10, No.2, February.

[9] T.F. Cootes and C.J. Taylor. 2001, Statistical models of appearance for computer vision. Technical report, Wolfson Image Analysis Unit, University of Manchester.